How to cite: Angew. Chem. Int. Ed. 2024, e202417170
doi.org/10.1002/anie.202417170

Boranes

# Stabilization of Ethane-Like Dianionic Diborane(6) in Monometallic Titanium Complexes and its Subsequent B($sp^3$)–B($sp^3$) Bond Cleavage

*Subhash Bairagi, Soumen Giri, Gaurav Joshi, Eluvathingal D. Jemmis,* and Sundargopal Ghosh**

**Abstract:** Treatment of [Cp*$TiCl_3$] with [$LiBH_4$·THF] followed by thermolysis with [$Ph_2E_2$] (E=S or Se) resulted in the formation of classical diborane(6) complexes, [(Cp*Ti)($\eta^4$-$B_2H_4$LL′)] (L=$C_6H_4$E; L′=$C_6H_5$E; **1a**: E=S, **1b**: E=Se), stabilized at titanium template. To the best of our knowledge, they are the first examples of mono-metallic classical diborane(6) complexes. The bonding analysis and theoretical studies suggest that the stabilization of these diborane(6) species is due to the presence of four bridging ligands in $\kappa^4$-fashion, where two of them are phenyl thiolates/selenolates that provide more electrons to the electron-deficient titanium center. Reactions of these diborane(6) species with [M-$(CO)_5$·THF] (M=Mo, W) led to the cleavage of the electron-precise B($sp^3$)–B($sp^3$) bond that yielded $\kappa^3$-hydridoborato complexes [(Cp*Ti)($\kappa^3$-$BH_3$R)($\mu$-EPh)$_2$-{$M(CO)_4$}] (**2a–c**: R=H, **3a–c**: R=Ph). In an attempt to isolate the Te-analogue of **1a–b**, a similar reaction was performed; however, the complex was too unstable to be isolated. Interestingly, the treatment of this unstable intermediate with [$W(CO)_5$·THF] yielded [(Cp*Ti)($\kappa^3$-$BH_3$R)($\mu$-$TePh)_2${$W(CO)_4$}] (**2d**: R=H, **3d**: R=Ph) that are analogues of **2a–c** and **3a–c**, respectively. Formation of these species provide indirect evidence for the existence of unstable [(Cp*Ti)($\eta^4$-$B_2H_4$LL′)] (L=$C_6H_4$Te; L′=$C_6H_5$Te; **1c**).

Despite many dramatic advances in the chemistry of quintessential electron-deficient diborane, $[B_2H_6]$,[1–7] its electron-sufficient dianionic isomer,[8–12] $[B_2H_6]^{2-}$, is much less studied. Unlike ethane, isoelectronic $[B_2H_6]^{2-}$ cannot be isolated as a free species and can only be stabilized in transition metal-template.[8–10] In most of the complexes, $[B_2H_6]^{2-}$ acts as an effective ligand via bis(bidentate) chelation to form [$\kappa^4$-$B_2H_6$]$^{2-}$ metal complex with a tetrahedral unit of complex type **I** (Figure 1).[8] The first bimetallic classical diborane(6) complex, [$Fe_2(CO)_6$($\mu$-$\kappa^4$-$B_2H_6$)], spectroscopically characterized by Fehlner et al. in 1978, is isoelectronic to [$C_2H_2Co_2(CO)_6$].[8a] Subsequently, Cotton and co-workers described the structural characterization of complex **I**, which comprises a [$\kappa^4$-$B_2H_6$]$^{2-}$ ligand.[9a] It is noteworthy to mention that a few structurally characterized bis(bidentate) dianionic $[B_2H_6]^{2-}$ complexes having eclipsed conformation are known.[8] Apart from this bimetallic bis(bidentate) complex, a trimetallic tris(bidentate) complex (**II**), featuring eclipsed conformation is also known, where [$\kappa^6$-$B_2H_6$]$^{2-}$ utilized all of its hydrogen atoms to form three pairs of B–H–M bonds.[10] Given these fundamental developments, it is rather surprising that simple mono-metallic transition metal diborane(6) complexes comprising an ethane-like classical form of $[B_2H_6]^{2-}$ have not been known to date.

Recently, Braunschweig,[7c,13] Himmel,[14] and us[4b,c,7d,15] have individually developed diborane complexes, stabilized in transition-metal templates. In this regard, our group structurally characterized the first bimetallic diborane(4) complex, [{Cp*Mo-$(CO)_2$}$_2$($\mu$-$\eta^2$:$\eta^2$-$B_2H_4$)], where [$B_2H_4$] mimics the acetylene, [$C_2H_2$].[15a] Further, as shown in Figure 1 (**III**), we have recently reported a dithiolate-based diborane(5) species, stabilized in a bimetallic template, in

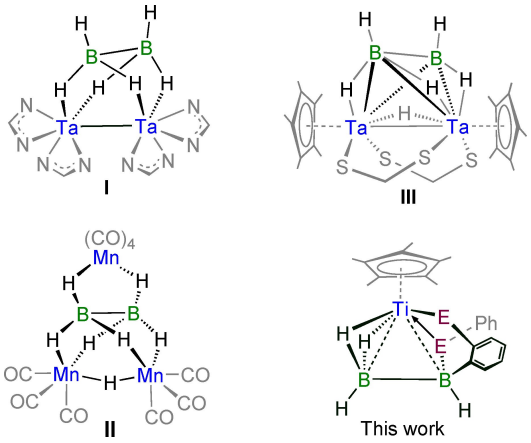


***Figure 1.*** Classical diborane(6) species stabilized in bi- (**I**: N=NR where R=*p*-tolyl, phenyl), tri- (**II**) and monometallic (This work: E=S or Se) frameworks, and classical diborane(5) in bimetallic (**III**) framework.

[*] S. Bairagi, S. Giri, Prof. S. Ghosh
Department of Chemistry
Indian Institute of Technology Madras
Chennai 600036, India
E-mail: sghosh@iitm.ac.in
G. Joshi, Prof. E. D. Jemmis
Inorganic and Physical Chemistry Department
Indian Institute of Science
Bangalore 560012, India
E-mail: jemmis@iisc.ac.in

which the classical $[B_2H_5]^-$ is the boron analogue of ethyl cation, $[C_2H_5]^+$.[15b] Added to these, the current thrust in stabilizing aromatic $[B_6H_6]^{6-}$ isoelectronic to benzene and other $[B_nH_n]^{n-}$ systems[16] motivated us to explore diborane chemistry by utilizing early transition metals to stabilize the ethane-like diborane(6) in a mononuclear complex. Herein, we present the first examples of monometallic classical diborane(6) derivatives $[(Cp^*Ti)(\kappa^4\text{-}B_2H_4LL')]$ (L=$C_6H_4E$; L′=$C_6H_5E$; **1a**: E=S, **1b**: E=Se), where diborane(6) exhibits as unique *tetrahapto* coordinated ligand $[\kappa^4\text{-}B_2H_4LL']$ in a mono-metallic template. Further, we have demonstrated the unusual reactivity of these diborane(6) complexes **1a–b**, where the B–B bond is elongated due to the donation of its 2e to the metal, with $[M(CO)_5\cdot THF]$ (M=Mo, W) that led to the formation of $\kappa^3$-borate complexes **2a–c** and **3a–c** through the cleavage of electron-precise B($sp^3$)–B($sp^3$) bond of the diborane(6) moiety.

The reaction of $[Cp^*TiCl_3]$ with three equivalents of $[LiBH_4\cdot THF]$ at −78 °C followed by thermolysis at 90 °C in presence of an excess of $[Ph_2E_2]$ (E=S, Se) resulted in the formation of $[(Cp^*Ti)(\kappa^4\text{-}B_2H_4LL')]$ (L=$C_6H_4E$; L′=$C_6H_5E$; **1a**: E=S, 52 % yield; **1b**: E=Se, 46 % yield; Scheme 1).[17] Complexes **1a–b** were isolated as purple solids, which were characterized by $^1$H, $^{11}$B{$^1$H}, $^{13}$C{$^1$H} NMR, IR, and UV/Vis spectroscopy, mass spectrometry, and single-crystal X-ray analysis. The $^1$H NMR spectra exhibited peaks at $\delta$=2.11 (**1a**) and 2.14 (**1b**) ppm that correspond to Cp* protons and the peaks at $\delta$=−1.43 (**1a**) and −1.37 (**1b**) indicative of Ti-*H*-B hydrogens. The room-temperature $^{11}$B{$^1$H} NMR spectra of **1a–b** displayed two resonances at $\delta$=−6.3 and 22.0 ppm (**1a**), and −1.8 and 23.4 ppm (**1b**), indicating two chemically inequivalent boron atoms. Additionally, the analysis of $^1$H{$^{11}$B} and $^1$H–$^{11}$B{$^1$H} HSQC NMR spectra facilitated the assignments of the terminal ($BH_t$) and bridging (Ti-*H*-B) hydrogen atoms. For instance, the $^1$H chemical shifts at $\delta$=−1.43 (**1a**) and −1.37 (**1b**) ppm correspond to Ti-*H*-B bridging hydrogens, attributed to the hydrogens linked to the boron that appeared at $\delta$=22.0 (**1a**) and 23.4 (**1b**) ppm in the $^{11}$B NMR. Similarly, the other boron atoms that appeared at $\delta$=−6.3 (**1a**) and −1.8 (**1b**) ppm are connected to only $BH_t$ hydrogens. The $^{13}$C{$^1$H} NMR spectra also confirmed the presence of Cp* and phenyl ligands. The $^{77}$Se NMR spectrum of **1b** showed two resonances at $\delta$=114.6 and 292.9 ppm that suggest the presence of two chemically inequivalent selenium atoms. The mass spectra displayed isotopic distribution patterns at *m/z* 427.1336 (**1a**) and 521.0395 (**1b**).

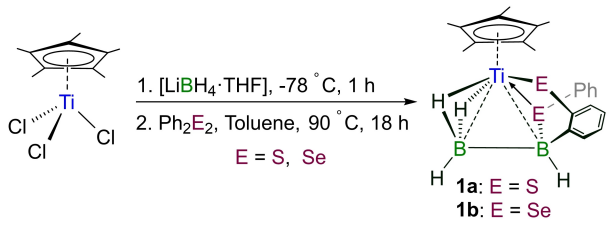


***Scheme 1.*** Synthesis of phenyl thiolate/selenolate-based titanium diborane(6) complexes **1a–b** (yield; **1*a*** = 52 %; **1*b*** = 46 %).

To validate the spectroscopic data and determine the solid-state X-ray structures of **1a–b**, single-crystal X-ray diffraction analyses were performed. The solid-state X-ray structures of **1a–b** revealed a classical diborane derivatives, unsymmetrically coordinated with {Cp*Ti} fragment through a $\kappa^4$-bridged fasion forming four-legged piano-stool type complexes (Figure 2). In the diborane moiety, B2 atom is bonded to the Ti center via two 3c–2e B–H–Ti bonds, while B1 atom is connected to the Ti center through two phenyl thiolate/selenolate groups (Figure S1). Among the two phenyl thiolate/selenolate ligands, one forms a covalent B–S/Se bond and a coordinate bond between the S/Se atom and the Ti center, while the other ligand forms a covalent B–C bond and another covalent bond between the S/Se atom and the Ti center. A notable feature of **1a–b** is the activation of the C–H bond of EPh (E=S or Se) ligand that led to B–C bond formation. The B–C bond lengths in **1a** (1.590(8) Å) and **1b** (1.586(7) Å) are comparable to that of reported C–H and B–H activated complexes $[(TaCp^*)_2B_5H_{10}(C_6H_5)]$[18a] (1.574(10) Å). However, they are slightly shorter as compared to $[(TaCp^*)_2(\mu\text{-}B_2H_4S)\{\mu\text{-}S\text{-}(C_6H_4)BH_3\}]$ (1.643(14) Å).[18b]

The presence of two phenyl thiolate or selenolate moieties linked with one of the boron atoms (B1) of the diborane unit is such that the Cp* ligand oriented to the opposite side of this particular boron atom to avoid steric hindrance. These unsymmetrical ligands around B1 (Figure 2) caused deviation from the eclipsed orientation of the ligands attached to the boron atoms (torsion angle $H_t$–B1–B2–$H_t$ ~18.32° (**1a**), 44.43° (**1b**)), unlike to the situation observed in classical diborane(6) molecules.[8–10] This led to lengthening of the Ti1-B1 distances (2.464(6) Å (**1a**) and 2.499(5) Å (**1b**)). In contrast, the Ti1–B2 distances of 2.109(7) Å (**1a**) and 2.105(6) Å (**1b**) are significantly shorter as compared to the Ti–B bond lengths in complexes $[(Cp^*Ti)_2(\mu_2\text{-}\kappa^4\text{-}B_2H_6)_2]$ (*av.* 2.387 Å), $[(Cp^*Ti)_2(\mu\text{-}B_6H_6)(\mu\text{-}H_6)]$[16a] (*av.* 2.316 Å) and $[(Cp^*Ti)_2B_{14}H_{18}]$[19] (*av.* 2.411 Å). The X-ray structures also display significantly longer B–B bond lengths of 1.855(8) Å (**1a**) and 1.808(8) Å (**1b**) that indicate the presence of B($sp^3$)–B($sp^3$) bond. Although the

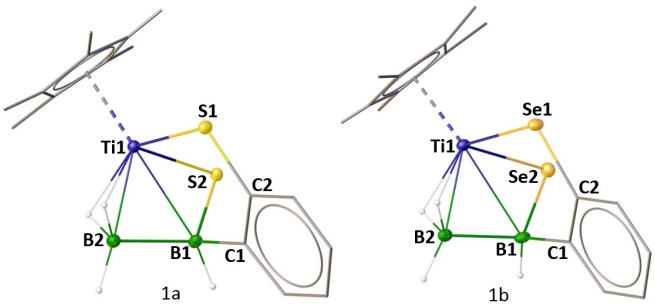


***Figure 2.*** Molecular structures and labelling diagrams of **1a–b**.[20] Ph-ligands attached to S2 and Se2 atoms and H-atoms of Cp* and Ph ligands are omitted for clarity. Selected bond lengths (Å) and angles (deg); **1a**: B1···Ti1 2.464(6), B2···Ti1 2.109(7), B1–B2 1.855(8), B2–$H_t$ 1.14(4), B2–$H_b$ 1.17(4),1.19(4), B1–C1 1.590(8), B1–S2 1.957(6), Ti1–$H_b$ 1.82(4), 1.88(4), Ti–S2 2.4186(15), B1–Ti1–B2 46.2(4); **1b**: B1···Ti1 2.499(5), B2···Ti1 2.105(6), B1–B2 1.808(8).

observed B–B distances are similar to $[H_3B–BH_3]^{2-}$ species, observed in $[(Cp^*Ti)_2(\mu_2\text{-}\kappa^4\text{-}B_2H_6)_2]$ (1.800(5) Å), they are considerably longer as compared to **III** (1.681(6) Å), shown in Figure 1. A qualitative electron counting Scheme suggests **1a–b** to a be 14 electron system ($Cp^{*-}$ (6e) + $[B_2H_4LL']^{2-}$ (4e from 2B–H bonds) + $[(C_6H_4)E]^-$ (2e) + $[(C_6H_5)E]$ (2e)), and $Ti^{4+}$ (zero e), where Ti is in +4 oxidation state. However, an AdNDP analysis shows **1a–b** to be an 18e complex, as seen below.

The intriguing bonding aspect of **1a–b** is investigated using DFT at the B3LYP-D3/Def2-SVP level. The optimized geometry at this level closely follows the X-ray structures (Table S2). We have performed the Adaptive Natural Density Partitioning (AdNDP)[21] analysis to generate a localized bonding picture of **1a** (Figure 3) and **1b** (Figure S66). The total 69 localized orbitals, corresponding to 138 valence electrons, are categorized into two lone pairs, one on each of the sulfur, 55 two centre-two electron (2c–2e), 3 three centre-two electron (3c–2e), and 9 six centre-two electron bonds. Among the 55 2c–2e are 22 C–C, 24 C–H, 2 B–H, 2 C–S, 1 B–S, 1 B–C, and 3 Ti–S bonds. Normally a lone pair count of two is anticipated on each sulfur. One lone pair on each sulfur is used to form additional 2c–2e bonds. In addition to the anticipated 2c–2e Ti–S1 sigma bond, there is a π-type Ti–S1 2c–2e bond. Similarly, the S2 forms two 2c–2e bonds, one each with B and Ti. This also accounts for the three Ti–S 2c–2e bonds. The three 3c–2e bonds are B2-H4-Ti1, B2-H3-Ti1, and Ti1-B1-B2. The two benzene rings account for six 6c–2e π-bonds; the remaining three 6c–2e bonds arise from the π-orbitals of cyclopentadienyl with titanium. The 3c–2e Ti1–B1–B2 bond involving the donation of B–B sigma bond of a saturated $[B_2H_6]^{2-}$ derivative to the metal is rare (Figure 3). This 3c–2e bond between the metal and two boron atoms makes the B–B bond weak; Wiberg bond index is only 0.68. The interaction of the two boron with the metal is not symmetrical. The 3c–2e bond has slightly more coefficients on {$BH_3$} boron (33 %) than {BHLL′} boron (29 %). Also, the {$BH_3$} boron has additional two 3c–2e interaction with metal and bridging hydrogens H3 and H4, signifying its close contact with metal than the {BHLL′} boron (Figure 3). Wiberg bond Indices further support this argument (Ti1–B1 = 0.28, Ti1–B2 = 0.64). Another interesting feature is the difference in bonding between Ti and S1/S2. The longer distance S2 has only a 2c–2e σ-bond, while the shorter S1 also has a π-bonding, signifying the bond's coordinative nature in the former (Figure 3). The 2e donation from the B–B bond and the 2e from the S1 of $C_6H_4S1$ for the Ti–S1 π-bond make **1a** a formal 18e complex. The synthesis of isostructural **1a** and **1b** with a formal $[B_2H_6]^{2-}$ ligand starting from $[LiBH_4]$ is also an indicator of the extra stability of this 18e arrangement.

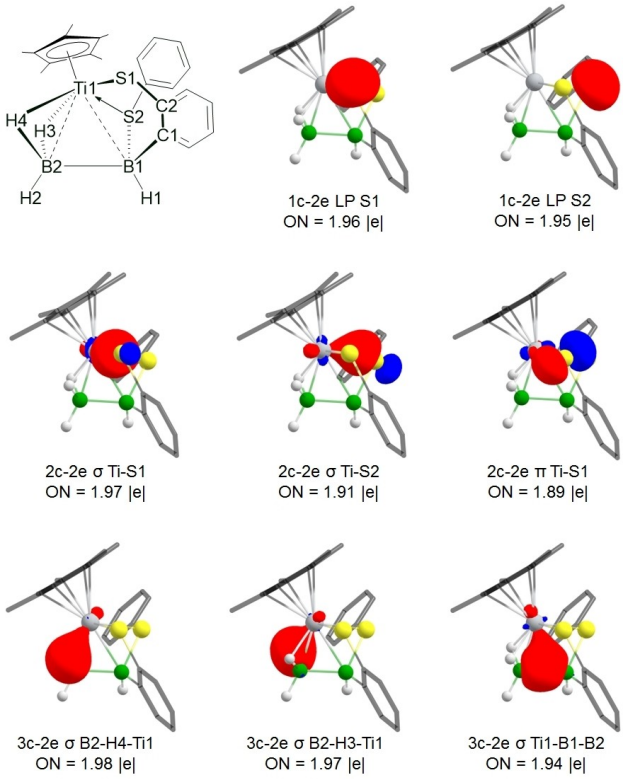


***Figure 3.*** Selected localized orbitals of **1a** (see text). The occupancy threshold of 1.8 is used for the selection of candidate localized orbitals.

The interaction of boranes with transition-metal centers has been a prime aspect of our research.[4b,c,7d,15,16a] Given their widespread applications in catalysis, these investigations have centered on the interaction of the B–H and B–B bonds with metals.[1,2] In this regard, the diboration reaction is notable as "the most-used organometallic reaction in organic synthesis" involving diborane. This provides a valuable synthetic method for introducing a boryl group into an unsaturated organic compound.[2a] Diborane species are also important starting materials to generate electron-precise metal–boron bonds.[2b,c,22] Braunschweig et al. described the cleavage of the B–B bond in diborane(4) that led to the formation of borylene complex $[(C_5H_4Me)Mn(CO)_2]_2(\mu\text{-}BX)]$ (X=$NMe_2$, $^t$Bu).[22a] Later, Shimoi group showed the fragmentation of $[B_2H_4\cdot 2PMe_3]$ that generated a boron analogue of methylene, $[BH\cdot PMe_3]$, which was stabilized as a bridging ligand in $[\{Co(CO)_3\}(\mu\text{-}CO)(\mu\text{-}BH\cdot PMe_3)]$.[22b] Note that the experimental and theoretical studies suggest a longer and weaker B–B bond in **1a–b**. Intrigued by these findings, we sought to explore the reactivity of **1a–b** toward $[M(CO)_5\cdot THF]$ (M=Mo, W) that led to the cleavage of B–B bond and yielded $\kappa^3$-hydridoborato complexes, $[(Cp^*Ti)(\kappa^3\text{-}BH_3R)(\mu\text{-}EPh)_2\{M(CO)_4\}]$ (**2a–c**: R=H; **3a–c**: R=Ph; Scheme 2(a)). Note that these reactions also yielded other air and moisture sensitive products in low yields. The reaction mixtures were separated using thin layer chromatography (TLC) on aluminium-supported silica gel plates. Although elution with hexane and dichloromethane solvent (80:20 v/v) allowed us to isolate **2a–c** and **3a–c** as green solids, all of our attempts to isolate other species were unsuccessful. Compounds **2a–c** and **3a–c** were characterized by $^1$H, $^{11}$B{$^1$H}, $^{13}$C{$^1$H} NMR, IR, and UV/Vis spectroscopy, mass spectrometry, and single-crystal X-ray analysis.

After the successful isolation of these hydridoborato species, we now tried to isolate the Te-analogues of **2a–c**

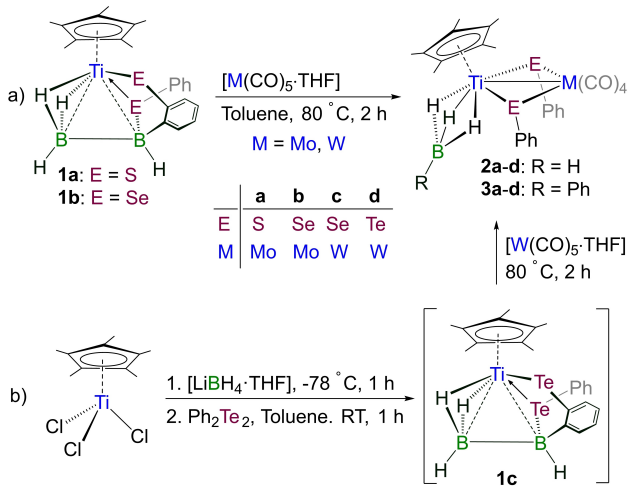


***Scheme 2.*** Synthesis of borate complexes **2a–d** and **3a–d** having $\kappa^3$-$BH_3R$ (R=H, Ph) ligands (yield; **2*a*** = 42%; **2*b*** = 44%; **2*c*** = 37%; **2d** = 23%; **3*a*** = 25%; **3*b*** = 23%; **3*c*** = 20%; **3d** = 11%). **1c** represents the possible intermediate, Te-analogue of **1a–b**.

and **3a–c**. As a result, we treated the in situ generated intermediate, obtained from the reaction of $[Cp^*TiCl_3]$, $[LiBH_4{\cdot}THF]$ and $[Ph_2Te_2]$, with $[W(CO)_5.THF]$ (Scheme 2-(b)) that indeed led to the formation of hydridoborato species, $[(Cp^*Ti)(\kappa^3\text{-}BH_3R)(\mu\text{-}TePh)_2\{W(CO)_4\}]$ (**2d**: R=H; **3d**: R=Ph). Complexes **2d** and **3d** were also isolated as green solids, which were characterized by various spectroscopic data and single-crystal X-ray analysis. Thus, the structural isolation of $\kappa^3$-hydridoborato complexes **2d** and **3d** indirectly suggest the existence of the Te-analogue of **1a–b**, that is $[(Cp^*Ti)(\eta^4\text{-}B_2H_4LL')]$ (L=$C_6H_4Te$; L′=$C_6H_5Te$; **1c**).

The $^{11}B\{^1H\}$ NMR spectra of **2a–d** and **3a–d** displayed a single set of resonances in the range of $\delta$ = 4.6–17.1 ppm, suggesting the presence of tetra-coordinated boron atoms. Note that the $^{11}B$ chemical shifts for **2a–d** as well as **3a–d** are shifted downfield while moving from S→Se→Te (S: δ = 4.6 (**2a**), 12.8 (**3a**); Se: $\delta$ = 6.5 (**2b**), 14.9 (**3b**); and Te: δ = 8.9 (**2d**), 17.1 (**3d**) ppm). The $^1H$ chemical shifts of the B-*H*-Ti bridging hydrogens were similar to that of diboranes species **1a–b**. The $^1H$ and $^{13}C\{^1H\}$ NMR spectra further confirmed the presence of both Cp* and Ph ligands. The $^{77}Se$ chemical shifts for complexes **2b** and **3b** appeared as singlets at $\delta$ = 742.4 and 734.0 ppm, respectively that suggest chemically equivalent selenium atoms. The IR spectra of **2a–d** showed absorption bands associated with CO (terminal), B–H (terminal), and B–H (bridging) bonds. While **3a–d** show absorption bands corresponding to only terminal CO and bridging B–H stretches. Furthermore, the mass spectra of complexes **2a–d** and **3a–d** suggest molecular formulas of $C_{26}H_{29}BO_4E_2TiM$ and $C_{32}H_{33}BO_4E_2TiM$, respectively. To validate the spectroscopic data and determine the solid-state X-ray structures of these species, the single-crystal X-ray diffraction analyses were performed. The solid-state X-ray structures of **2a–b**, **2d**, and **3b–d** are shown in Figures 4, 5, and S2–S4.

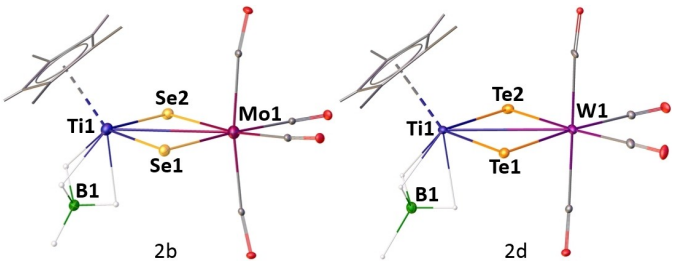


***Figure 4.*** Molecular structures and labelling diagrams of **2b** and **2d**.[19] Hydrogen atoms of Cp* ligands and Ph ligands attached to chalcogen atoms are omitted for clarity. Selected bond lengths (Å) and angles (deg); **2b**: B1···Ti1 2.149(6), B1–$H_t$ 1.14(4), B1–$H_b$ 1.06(5)–1.23(5), Ti1–$H_b$ 1.85(5)–1.98(5), Ti1–Mo1 3.2172(9), Ti1–Se1–Mo1 76.25(3); **2d**: B1···Ti1 2.165(11), Ti1–$H_b$ 1.87(7)–2.00(7), Ti1–W1 3.2689(16), Ti1–Te1 2.7295(15), Ti1–Te1–W1 72.07(3).

The molecular structures of **2b**, **2d** (Figure 4), and **3b**, **3d** (Figure 5) clearly show that a hydridoborato $[BH_3R]^-$ (R=H, Ph) moiety is attached to Cp*Ti fragment in $\kappa^3$-fashion. Additionally, a $\{M(CO)_4\}$ (M=Mo and W) fragment is bonded to the Ti center through two chalcogen bridges forming a flattened butterfly core of $[TiME_2]$. One of the striking features of **2a–d** and **3a–d** is the presence of $\kappa^3$-coordinated $BH_3R$ (R = H, Ph) ligand. The presence of a linear Ti-B–R skeleton (167.9(4)–178.2(5)°), three short Ti–H distances (1.82(3)–2.05(3) Å), and associated short Ti–B distance (2.149(6)–2.168(5) Å) suggest a $\kappa^3$-$BH_3R$–Ti interaction. The Ti···B distances are similar to those observed for the $\kappa^3$-hydridoborato ligands in $[(CO)_4Ti(\kappa^3\text{-}BH_4)]$[23a] (2.158(7) Å) and $[\{(Cp^*Ti)(\kappa^3\text{-}BH_3Me)\}_2(\mu\text{-}B_2H_6)]$[9c] (2.162(3) and 2.170(3) Å).[23b] The coordinated $\kappa^3$-hydridoborato ligand is essentially tetrahedral with B-$H_b$ distances of 1.06(5)–1.23(5) Å. Additionally, all the H–B–H angles fall within the narrow range of tetrahedral structure, consistent with a relatively unperturbed tetrahedral $\kappa^3$-$BH_3R$ ligand.[23a,b] On the other hand, the $[TiME_2]$ butterfly core, similar to that of $[\{(CO)_4M(SePh)_2\}Cp^*Ta\{B_4H_8\}]$[23c]

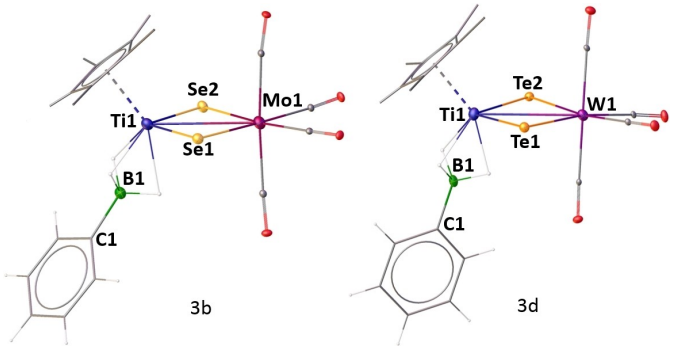


***Figure 5.*** Molecular structures and labelling diagrams of **3b** and **3d**.[19] Hydrogen atoms of Cp* ligands and Ph ligands attached to chalcogen atoms are omitted for clarity. Selected bond lengths (Å) and angles (deg); **3b**: B1···Ti1 2.165(5), Ti1–$H_b$ 1.84(4)–2.05(3), B1–C1 1.568(6), Ti1–Se1–Mo1 75.861(19); **3d**: B1···Ti1 2.158(7), Ti1–$H_b$ 1.864–1.935, B1–C1 1.564(9), Ti1–Te1–W1 72.40(2).

(M=Mo, W), comprised 38 valence electrons. Although the oxidation states of Ti and group 6 metals of (+4) and (0), respectively, remained unaffected, an increase of 2e at the Ti centers at **2a–d** and **3a–d** has been observed.

In summary, we have synthesized and structurally characterized ethane-like dianaionic diborane(6) species in a monometallic template of titanium, where the diborane moiety bridges the metal center by a novel $\kappa^4$-coordination mode. Detailed theoretical studies provide insight into the rationale behind the stabilization of diborane(6) species in the monometallic template where the presence of a 3c–2e Ti–B–B bonding interaction weakens the B–B bond in diborane moiety. Additionally, we have demonstrated the reactivity of the diborane(6)-metal complex towards group 6 metal fragments, which perturbs the B–B bond and resulted in $\kappa^3$-hydridoborato complexes. Further utilization of these hetero-dinuclear borate complexes in dehydrogenation, catalytic hydroboration, and C–H functionalization reactions is currently underway, and we expect further developments in the near future.

## Acknowledgements

The generous support of SERB, New Delhi, India (grant no. CRG/2023/000189) is gratefully acknowledged. S.B thanks IIT Madras, S.G thanks UGC and G.J. thanks IISc for research fellowships. We thank Dr. Elias Jesu Packiam, IIT Madras, for the X-ray structure analyses. The computational facility of SERC-IISc is gratefully acknowledged.

## Conflict of Interest

The authors declare no conflict of interest.

## Data Availability Statement

The data that support the findings of this study are available in the supplementary material of this article.

**Keywords:** Diborane · Classical · Borate · Titanium · Chalcogen

[1] a) I. A. I. Mkhalid, J. H. Barnard, T. B. Marder, J. M. Murphy, J. F. Hartwig, *Chem. Rev.* **2010**, *110*, 890–931; b) R. D. Dewhurst, E. C. Neeve, H. Braunschweig, T. B. Marder, *Chem. Commun.* **2015**, *51*, 9594–9607; c) E. C. Neeve, S. J. Geier, I. A. I. Mkhalid, S. A. Westcott, T. B. Marder, *Chem. Rev.* **2016**, *116*, 9091–9161; d) A. J. J. Lennox, G. C. Lloyd-Jones, *Chem. Soc. Rev.* **2014**, *43*, 412–443; e) C. F. Lane, *Chem. Rev.* **1976**, *76*, 773–779; f) C. Kojima, K.-H. Lee, Z. Lin, M. Yamashita, *J. Am. Chem. Soc.* **2016**, *138*, 6662–6669.

[2] a) S. K. Ritter, *Chem. Eng. News* **2016**, *94*, 5; b) G. J. Irvine, M. J. G. Lesley, T. B. Marder, N. C. Norman, C. R. Rice, E. G. Robins, W. R. Roper, G. R. Whittell, L. J. Wright, *Chem. Rev.* **1998**, *98*, 2685–2722; c) S. A. Westcott, E. Fernández, *Adv. Organomet. Chem.* **2015**, *63*, 39–89.

[3] a) W. Siebert, *In Advances in Boron Chemistry*, The Royal Society of Chemistry, Cambridge, **1997**; b) V. M. Dembitsky, H. A. Ali, M. Srebnik, *Adv. Organomet. Chem.* **2004**, *51*, 193–250; c) P. P. Power, *Chem. Rev.* **1999**, *99*, 3463–3504; d) Y. Wang, G. H. Robinson, *Chem. Commun.* **2009**, 5201–5213.

[4] a) J. D. Kennedy, *Prog. Inorg. Chem.* **2007**, *32*, 519–679; b) R. Borthakur, K. Saha, S. Kar, S. Ghosh, *Coord. Chem. Rev.* **2019**, *399*, 213021; c) R. Bag, S. Bairagi, B. K. Rout, S. Ghosh, in *Encyclopedia of Inorganic and Bioinorganic Chemistry*, (Ed. R. Melen), Wiley, **2022**.

[5] a) K. H. K. Reddy, E. D. Jemmis, *Dalton Trans.* **2013**, *42*, 10633–10639; b) T. J. Coffy, G. Medford, J. Plotkin, G. J. Long, J. C. Huffman, S. G. Shore, *Organometallics* **1989**, *8*, 2404–2409.

[6] A. Stock, in *Hydrides of Boron and Silicon*, Cornell University Press, Ithaca, N. Y., **1933**.

[7] a) G. Medford, S. G. Shore, *J. Am. Chem. Soc.* **1978**, *100*, 3953–3954; b) J. Feilong, T. P. Fehlner, A. L. Rheingold, *J. Organomet. Chem.* **1988**, *348*, C22–C26; c) S. R. Wang, D. Prieschl, J. D. Mattock, M. Arrowsmith, C. Pranckevicius, T. E. Stennett, R. D. Dewhurst, A. Vargas, H. Braunschweig, *Angew. Chem. Int. Ed.* **2018**, *57*, 6347–6351; d) R. S. Anju, D. K. Roy, B. Mondal, K. Yuvaraj, C. Arivazhagan, K. Saha, B. Varghese, S. Ghosh, *Angew. Chem. Int. Ed.* **2014**, *53*, 2873–2877.

[8] a) E. L. Andersen, T. P. Fehlner, *J. Am. Chem. Soc.* **1978**, *100*, 4606–4607; b) S. Aldridge, M. Shang, T. P. Fehlner, *J. Am. Chem. Soc.* **1998**, *120*, 2586–2598; c) X. Lei, M. Shang, T. P. Fehlner, *J. Am. Chem. Soc.* **1999**, *121*, 1275–1287.

[9] a) F. A. Cotton, L. M. Daniels, C. A. Murillo, X. Wang, *J. Am. Chem. Soc.* **1996**, *118*, 4830–4833; b) H. Brunner, G. Gehart, W. Meier, J. Wachter, B. Wrackmeyer, B. Nuber, M. L. Ziegler, *J. Organomet. Chem.* **1992**, *436*, 313–324; c) E. D. Horno, J. Jover, M. Mena, A. Pérez-Redondo, C. Yélamos, *Chem. Eur. J.* **2022**, *28*, 20210308.

[10] a) H. D. Kaesz, W. Fellmann, G. R. Wilkes, L. F. Dahl, *J. Am. Chem. Soc.* **1965**, *87*, 2753–2755; b) R. Prakash, A. N. Pradhan, M. Jash, S. Kahlal, M. Cordier, T. Roisnel, J.-F. Halet, S. Ghosh, *Inorg. Chem.* **2020**, *59*, 1917–1927.

[11] a) A. Stock, H. Z. Laudenklos, *Anorg. Allg. Chem.* **1936**, *228*, 178–192; b) W. J. Grigsby, P. P. Power, *J. Am. Chem. Soc.* **1996**, *118*, 7981–7988.

[12] a) Y. Shoji, T. Matsuo, D. Hashizume, M. J. Gutmann, H. Fueno, K. Tanaka, K. J. Tamao, *Am. Chem.* **2011**, *133*, 11058–11061; b) T. Kaese, A. Hübner, M. Bolte, H.-W. Lerner, M. Wagner, *J. Am. Chem. Soc.* **2016**,*138*, 6224–6233.

[13] M. Arrowsmith, H. Braunschweig, T. E. Stennett, *Angew. Chem. Int. Ed.* **2017**, *56*, 96–115.

[14] a) A. Wagner, E. Kaifer, H.-J. Himmel, *Chem. Commun.* **2012**, *48*, 5277–5279; b) A. Wagner, E. Kaifer, H.-J. Himmel, *Chem. Eur. J.* **2013**, *19*, 7395–7409.

[15] a) B. Mondal, R. Bag, S. Ghorai, K. Bakthavachalam, E. D. Jemmis, S. Ghosh, *Angew. Chem. Int. Ed.* **2018**, *57*, 8079–8083; b) K. Saha, S. Ghorai, S. Kar, S. Saha, R. Halder, B. Raghavendra, E. D. Jemmis, S. Ghosh, *Angew. Chem. Int. Ed.* **2019**, *58*, 17684–17689.

[16] a) S. Kar, S. Bairagi, A. Haridas, G. Joshi, E. D. Jemmis, S. Ghosh, *Angew. Chem. Int. Ed.* **2022**, *61*, e202208293; b) V. R. Miller, R. N. Grimes, *J. Am. Chem. Soc.* **1973**, *95*, 5078–5080; c) R. Weiss, R. N. Grimes, *J. Am. Chem. Soc.* **1977**, *99*, 8087–8088; d) G. Joshi, E. D. Jemmis, *Chemistry-A Eur. J.* **2024**, *30*, e202402410; e) C. Luz, K. Oppel, L. Endres, R. D. Dewhurst, H. Braunschweig, U. Radius, *J. Am. Chem. Soc.* **2024**, *146*, 23741–23751.

[17] Under identical conditions using [$Ph_2Te_2$], no tellurium analogue of complexes **1a–b** was isolated.

[18] a) S. K. Bose, K. Geetharani, S. Ghosh, *Chem. Commun.* **2011**, *47*, 11996–11998; b) S. Kar, K. Kar, S. Bairagi, M. Bhattacharyya, M. G. Chowdhury, S. Ghosh, *Inorg. Chim. Acta* **2022**, *530*, 120685.
[19] S. Kar, S. Bairagi, J–F. Halet, S. Ghosh, *Chem. Commun.* **2023**, *59*, 11676–11679.
[20] CCDC 2307014 (**1a**), 2329838 (**1b**), 2343795 (**2a**), 2337833 (**2b**), 2356121 (**3b**), 2329839 (**3c**), 2379765 (**2d**) and 2379768 (**3d**) contain the supplementary crystallographic data for this paper. These data are provided free of charge by The Cambridge Crystallographic Data Centre.
[21] a) N. V. Tkachenko, A. I. Boldyrev, *Phys. Chem. Chem. Phys.* **2019**, *21*, 9590–9596; b) D. Y. Zubarev, A. I. Boldyrev, *Phys. Chem. Chem. Phys.* **2008**, *10*, 5207–5217.
[22] a) H. Braunschweig, T. Wagner, *Angew. Chem. Int. Ed.* **1995**, *34*, 825–826; b) M. Shimoi, S. Ikubo, Y. Kawano, *J. Am. Chem. Soc.* **1998**, *120*, 4222–4223.
[23] a) P. J. Fischer, V. G. Young Jr., J. E. Ellis, *Angew. Chem.* **2000**, *112*, 195–197; b) A. Calvo-Molina, E. del Horno, J. Jover, A. Pérez-Redondo, C. Yélamos, R. Zapata, *Organometallics* **2023**, *42*, 1360–1372; c) S. Kar, K. Kar, S. Ghosh, *Organometallics* **2022**, *41*, 1125–1129.

Manuscript received: September 6, 2024
Accepted manuscript online: October 30, 2024
Version of record online: ■■, ■■

# Communication

**Boranes**

S. Bairagi, S. Giri, G. Joshi, E. D. Jemmis,*
S. Ghosh* ——————— **e202417170**

Stabilization of Ethane-Like Dianionic Diborane(6) in Monometallic Titanium Complexes and its Subsequent B($sp^3$)–B($sp^3$) Bond Cleavage

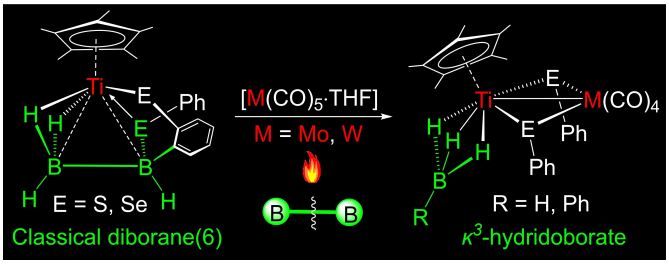


Ethane-like classical dianionic diborane(6) species stabilized by mononuclear Cp*Ti have been isolated and structurally characterized. Treatment of these diborane(6) species with [M(CO)$_5$·THF] (M = Mo or W) led to the cleavage of electron-precise B($sp^3$)–B($sp^3$) bonds that yielded $\kappa^3$-hydridoborato complexes (see picture).